Proc. Int. Symposium on Advances in Neutron Scattering Research, Tokai, 2000
J. Phys. Soc. Jpn. **70** (2001) Suppl. A pp. 121–123

# Diverse Magnetic Ground States in the Tetragonal $R^{11}B_2C_2$ (R=rare earth) System

Kenji OHOYAMA, Aya TOBO, Hiroki YAMAUCHI, Koji KANEKO, Kentaro INDOH, Hideya ONODERA, Yasuo YAMAGUCHI and Hiroaki KADOWAKI[1]

*Institute for Materials Research, Tohoku Univ., Sendai 980-8577, Japan*
[1] *Department of Physics, Tokyo Metropolitan Univ., Tokyo 192-0397, Japan*

Magnetic structures have been investigated in $R^{11}B_2C_2$ (R=rare earth) with the same tetragonal structure as that of the antiferroquadrupolar (AFQ) ordering compound $DyB_2C_2$ by powder diffraction technique. $R^{11}B_2C_2$ shows various and characteristic magnetic structures including long period structures, which are caused by competition among AFQ and antiferromagnetic interactions and magnetic anisotropy by the crystalline electric field effect.

KEYWORDS: $RB_2C_2$, antiferroquadrupolar ordering, magnetic structure, neutron powder diffraction

## §1. Introduction

$DyB_2C_2$ with the tetragonal $LaB_2C_2$ type crystal structure ($P4/mbm$ : La at 2($a$) site and B, C at 4($h$) site)[1] is the first compound which undergoes an antiferroquadrupolar (AFQ) ordering among tetragonal compounds with well-localised $4f$ states; it exhibits the AFQ ordering at $T_Q$=24.7 K and a further transition to an antiferromagnetic (AFM) state with a weak ferromagnetic component at $T_N$ =15.3 K.[2] Note that $T_Q$ of $DyB_2C_2$ is nearly ten times higher than those in other AFQ compounds, for instance, $T_Q$=1.8 K in TmTe[3] and $T_Q$=3.3 K in the Kondo compound, $CeB_6$.[4] The AFQ ordered state in $DyB_2C_2$ below $T_Q$ was confirmed by means of the resonant X-ray diffraction technique as well.[5,6]

Onodera *et al.* reported that the isostructural compound $HoB_2C_2$ also undergoes an AFQ ordering at $T_Q$=5.0 K.[7] The temperature dependence of magnetic susceptibility of $HoB_2C_2$ shows an apparent anomaly at $T_Q$, and a broad hump at $T_N$=5.8 K which is higher than $T_Q$. Since phase IV between $T_Q$ and $T_N$ is a magnetic ordered state, $HoB_2C_2$ is a new type AFQ material which exhibits the AFQ ordering in a magnetic ordered state.[7]

The AFQ orderings in $DyB_2C_2$ and $HoB_2C_2$ were confirmed from a characteristic magnetic structure: the angle between adjacent magnetic moments, which lie in the $c$-plane, along [0 0 1] is about 70°,[8] the magnetic moments in the $c$-plane make an angle of about 150° in each $c$-plane. Consequently, the magnetic structure has a periodicity of $2c$ along [0 0 1], where $c$ is the lattice constant. To describe the fundamental magnetic structure of $DyB_2C_2$ and $HoB_2C_2$, two propagation vectors of $\boldsymbol{k}_1$=[1 0 0], $\boldsymbol{k}_2$=[0 1 1/2] are needed, besides $\boldsymbol{k}_3$=[0 0 0] and $\boldsymbol{k}_4$=[0 0 1/2] for the canting structure in the $c$-plane. The multi-$\boldsymbol{k}$ structure in the AFQ compounds is thought to be caused by effects of competitive coexistence of AFQ and AFM interactions.[2,8] In other words, therefore, to understand roles of AFQ and AFM interactions for the magnetic properties, it is important to make clear and to compare the magnetic structures in the isostructural $RB_2C_2$ system. This work, thus, aims at determining the magnetic structures of $R^{11}B_2C_2$ by neutron diffraction technique. Some of the detailed results have been reported elsewhere.[2,8,9]

## §2. Experimental Details

For sample preparation, the mixtures of 99.9% pure R(R=Ce, Nd, Tb, Dy, Ho, Er and Tm), 99.5% pure $^{11}B$ and 99.999% pure C were melted by the conventional argon arc technique. To avoid strong absorption, natural boron was replaced with enriched $^{11}B$ isotope. Single crystals of $R^{11}B_2C_2$ grown by the Czochralski method with a tri-arc furnace were crushed into fine powder for neutron powder diffraction experiments.

We performed neutron powder diffraction experiments on the powder diffractometer for high efficiency and high resolution measurements, HERMES, belonging to Institute for Materials Research, Tohoku University, installed at the JRR-3M reactor in Japan Atomic Energy Research Institute, Tokai.[10] Neutrons with a wavelength of 1.8196Å were obtained by the Ge 3 3 1 monochromator and 12'-blank-sample-$\alpha_3$ collimation, where $\alpha_3$ was 22' for $R^{11}B_2C_2$(R=Ce, Nd, Tb, Dy, Ho and Tm), and 18' for $Er^{11}B_2C_2$.

## §3. Results and Discussion

Figures 1 show the powder patterns of $R^{11}B_2C_2$ (R=Dy, Ho, Tb, Nd, Er and Tm) in each ground state obtained on HERMES. Bragg peaks denoted with letter M are magnetic ones because the peaks do not exist in the paramagnetic states. As shown in Figs. 1, $R^{11}B_2C_2$ show various powder patterns in spite of the same crystal structure. Based on the obtained patterns, the compounds are classified into three groups: Upper: $Dy^{11}B_2C_2$ and $Ho^{11}B_2C_2$. Middle: $Tb^{11}B_2C_2$. Below: $Nd^{11}B_2C_2$, $Er^{11}B_2C_2$ and $Tm^{11}B_2C_2$.

The patterns of $Dy^{11}B_2C_2$ and $Ho^{11}B_2C_2$ in Figs. 1(a) and 1(b) are characterised by the strong M1 0 0 and M1 0 1/2 magnetic peaks with $\boldsymbol{k}_1$=[1 0 0], $\boldsymbol{k}_2$=[0 1 1/2]. These peaks and the weak M0 0 1/2 peak indicate the

TableI. Summary of the magnetic structures of $R^{11}B_2C_2$. In the table, $\boldsymbol{k}$ means propagation vectors for the magnetic structures and $\alpha_J$ are the Stevens' multiplicative factors. F and AF mean ferromagnetic and antiferromagnetic couplings, respectively.

| | $T_N$ | $T_Q$ | $\boldsymbol{k}$ | $\mu$ | $\alpha_J$ | Coupling along [1 1 0] | [0 0 1] |
|---|---|---|---|---|---|---|---|
| $Ce^{11}B_2C_2$ | 6.5 K,7.3 K[11] | | $[\delta\,\delta\,\delta']$ | $\mu \perp c$ | -0.0571 | F | F |
| $Nd^{11}B_2C_2$ | 8.0 K[9] | | $\boldsymbol{k}_1$ | $\mu//c$ | -0.0064 | AF | F |
| $Tb^{11}B_2C_2$ | 21.7 K[14] | | $\boldsymbol{k}_1$, $\boldsymbol{k}_{L2}$ | $\mu \perp c$ | -0.0101 | AF | AF |
| $Ho^{11}B_2C_2$ | 5.8 K[7] | 5.0 K[7] | $\boldsymbol{k}_1$,$\boldsymbol{k}_2$,$\boldsymbol{k}_3$,$\boldsymbol{k}_4$ | $\mu \perp c$ | -0.0064 | AF | 70° |
| *$Ho^{11}B_2C_2$ | | | $\boldsymbol{k}_1$,$\boldsymbol{k}_{L1}$ | $\mu \perp c$ | | AF | F |
| $Dy^{11}B_2C_2$ | 15.3 K[2] | 24.7 K[2] | $\boldsymbol{k}_1$,$\boldsymbol{k}_2$,$\boldsymbol{k}_3$,$\boldsymbol{k}_4$ | $\mu \perp c$ | -0.0022 | AF | 70° |
| $Er^{11}B_2C_2$ | 13.0 K 15.9 K[14] | | $\boldsymbol{k}_1$ | $\mu//c$ | 0.0025 | AF | F |
| *$Er^{11}B_2C_2$ | | | $\boldsymbol{k}_{L2}$ | $\mu//c$ | | AF | F |
| $Tm^{11}B_2C_2$ | 16.5 K[14] | | $\boldsymbol{k}_2$ | $\mu//c$ | 0.0101 | AF | AF |

$\boldsymbol{k}_1$=[1 0 0], $\boldsymbol{k}_2$=[0 1 1/2], $\boldsymbol{k}_3$=[0 0 0] and $\boldsymbol{k}_4$=[0 0 1/2], $\boldsymbol{k}_{L1}$=[1-$\delta$ $\delta$ $\delta'$], $\boldsymbol{k}_{L2}$=[1-$\delta$ $\delta$ 0]
* intermediate phase in $Ho^{11}B_2C_2$ at 5.3 K and $Er^{11}B_2C_2$ at 14 K

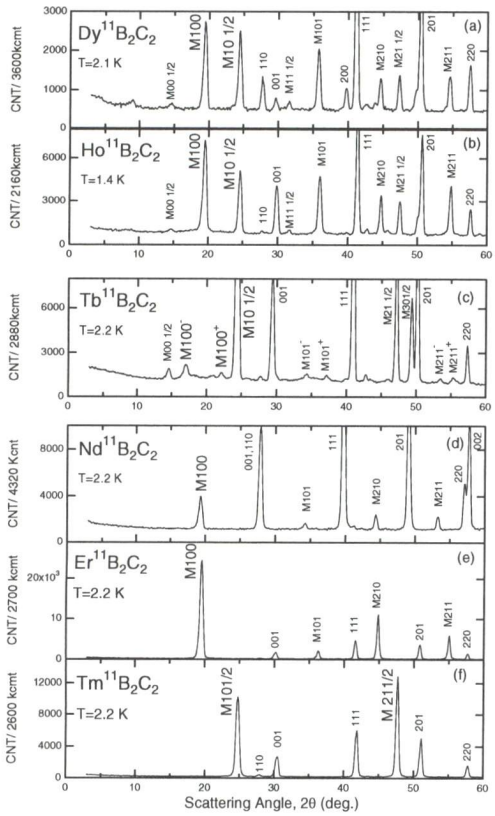


Fig. 1. Powder patterns of $R^{11}B_2C_2$ (R=Dy(a), Ho(b), Tb(c), Nd(d), Er(e) and Tm(f)) in the ground states observed on HERMES. Bragg peaks indexed with letter M are magnetic ones

characteristic magnetic structure.[2,8] Moreover, the pattern of $Tb^{11}B_2C_2$ in Fig. 1(c) shows weak satellite peaks M1 0 0$^{\pm}$ which are caused from a long periodic component, besides strong magnetic reflections with $\boldsymbol{k}_2$=[0 1 1/2]. Note that the long periodic component is based on the $\boldsymbol{k}_1$-type coupling as well, though it is not dominant. On the other hand, simple powder patterns of $Nd^{11}B_2C_2$, $Er^{11}B_2C_2$ and $Tm^{11}B_2C_2$ in Figs. 1(d), 1(e) and 1(f) indicate that the magnetic structures are simple AFM structures with single $\boldsymbol{k}$. The propagation vector of $Nd^{11}B_2C_2$ and $Er^{11}B_2C_2$ is $\boldsymbol{k}_1$=[1 0 0], while that of $Tm^{11}B_2C_2$ is $\boldsymbol{k}_2$=[0 1 1/2]. The magnetic moments in $Nd^{11}B_2C_2$, $Er^{11}B_2C_2$ and $Tm^{11}B_2C_2$ are parallel to the $c$-axis, while those in $Dy^{11}B_2C_2$, $Ho^{11}B_2C_2$ and $Tb^{11}B_2C_2$ lie in the $c$-plane.

The magnetic structures of $RB_2C_2$ are summarised in Table I. The first important feature of $RB_2C_2$ is the various and characteristic magnetic structures. The magnetic structures in this system show quite various combinations of magnetic couplings and propagation vectors. It should be pointed out that, in spite of the variety of the magnetic structures, $RB_2C_2$ except $Tm^{11}B_2C_2$ and $Ce^{11}B_2C_2$ exhibit Bragg peaks with $\boldsymbol{k}_1$=[1 0 0]. Moreover, even in $Tb^{11}B_2C_2$, there exists the weak $\boldsymbol{k}_1$=[1 0 0] component as satellite peaks. Since $Nd^{11}B_2C_2$ and $Er^{11}B_2C_2$ are simple [1 0 0] type AFM compounds without AFQ orderings,[9] we think that the $\boldsymbol{k}_1$=[1 0 0] type magnetic correlation is the fundamental one in this system; the coupling along the $c$-axis is ferromagnetic and that in the $c$-plane is antiferromagnetic. On the other hand, both ends of $RB_2C_2$ have no $\boldsymbol{k}_1$=[1 0 0] type component; $Ce^{11}B_2C_2$ shows a long period structure based on the ferromagnetic coupling, $Tm^{11}B_2C_2$ has a simple $\boldsymbol{k}_2$=[0 1 1/2] type AFM structure.

Since, in our preliminary experiments in $TbB_2C_2$, an AFQ ordered state probably exists under magnetic fields as well, effects of AFQ interactions can not be neglected even in the ground state in $TbB_2C_2$. We conclude, thus, that the diversity of the magnetic structures is caused by competition between AFQ and $\boldsymbol{k}_1$=[1 0 0] type AFM interactions. In $Dy^{11}B_2C_2$ and $Ho^{11}B_2C_2$, the $\boldsymbol{k}_1$=[1 0 0] type AFM ordering is strongly affected by coexistence of the AFQ ordering so that the 70° relation with $2c$ periodicity along the $c$-axis is realised.

Nextly, we discuss the direction of magnetic moments. Under the lowest order approximation of the crystalline electric field (CEF) theory, magnetic anisotropy can be mainly described with the second order CEF parameter $B_2^0$ which is proportional to the Stevens' multiplicative factor $\alpha_J$. Thus, when the sign of $\alpha_J$ is the same in rare earth compounds, the directions of the magnetic moments in the compounds must be the same. However, as shown in Table I, the directions of the magnetic moments in the ordered states are not consistent with the sign of $\alpha_J$: the magnetic moments of $R^{11}B_2C_2$(R=Ce,

Tb, Ho and Dy) with $\alpha_J < 0$ are perpendicular to the $c$-axis, while those of $Nd^{11}B_2C_2$ with $\alpha_J < 0$ are parallel to the $c$-axis, and those of $R^{11}B_2C_2$ (R=Er and Tm) with $\alpha_J > 0$ are perpendicular to the $c$-axis. This indicates that $B_2^0$ is not the leading term of the CEF hamiltonian in the $RB_2C_2$ system. Higher order terms must play important roles for the magnetic anisotropy, and the diverse magnetic structures in this system as well. The quantitative treatment of CEF, thus, is highly necessary.

Another important feature of the magnetic structures in $RB_2C_2$ is that some compounds show incommensurate magnetic structures with long periodicity. Figures 2 show the powder patterns of $Ho^{11}B_2C_2$ and $Er^{11}B_2C_2$ in the intermediate states.[7,8] For comparison, the pattern of $Tb^{11}B_2C_2$ in the ground state shown in Fig. 1(c) is also displayed. In the pattern of $Ho^{11}B_2C_2$ at 5.3 K, we observed M1 0 0 and its satellite peaks M1 0 $0^{\pm}$ as well. On the other hand, the pattern of $Er^{11}B_2C_2$ at 14 K in Fig. 1(c) reveals sharp M1 0 $0^{\pm}$ satellites without M1 0 0. The patterns indicate that the magnetic structure in the intermediate phase in $Ho^{11}B_2C_2$ can be described with combination of an incommensurate component and AFM one with $\boldsymbol{k}_1$=[1 0 0], while only one incommensurate component exists in $Er^{11}B_2C_2$. Although the magnetic moments of $Er^{11}B_2C_2$ are parallel to the $c$-axis, from the intensity simulation, we confirmed that the satellite peaks were not caused from an anti-phase domain structure. Note that the long periodic component in the three compounds are based on the $\boldsymbol{k}_1$=[1 0 0] coupling which is the same as the fundamental one in the ground states.

From single crystal diffraction experiments, the propagation vector of the long period component of $Ho^{11}B_2C_2$ was determined as $\boldsymbol{k}_{L1}$=[1-$\delta$ $\delta$ $\delta'$], where $\delta$=0.11 and $\delta'$=0.04,[8,12] while those of $Er^{11}B_2C_2$ and $Tb^{11}B_2C_2$ were determined as $\boldsymbol{k}_{L2}$=[1-$\delta$ $\delta$ 0] from the neutron powder diffraction experiments.[13] In $CeB_2C_2$ based on the ferromagnetic coupling, however, the propagation vector was determined as [$\delta$ $\delta$ $\delta'$] type with $\delta$=0.16, $\delta'$=0.10.

It should be emphasised that the positions of the satellite peaks in the three compounds are quite close. This means that the periodicity of the incommensurate structures is nearly the same though the directions are not exactly the same,[8,13] while the periodicity in real space of $CeB_2C_2$ is much shorter than those of the others. As mentioned above, an important character in $RB_2C_2$ is the various magnetic structures. The common periodicity in the incommensurate structures, however, may suggest that the long periodicity is caused by an influence of a common property in the $RB_2C_2$ system; structures of the Fermi surface, for instance.

## §4. Summary

An important feature of the $RB_2C_2$ system with the same $LaB_2C_2$ type structure is diversity of the characteristic magnetic structures because of competitive coexistence of AFQ and AFM interactions and magnetic anisotropy by the CEF effect. This suggests that, to understand mechanism of AFQ orderings, study of properties in only $DyB_2C_2$ and $HoB_2C_2$ is not enough, but it is indispensable to understand and to compare the magnetic properties in this system as a whole. To make clear the magnetic structures and dynamic properties, neutron elastic and inelastic scattering experiments with high-quality single crystalline samples are now in progress.

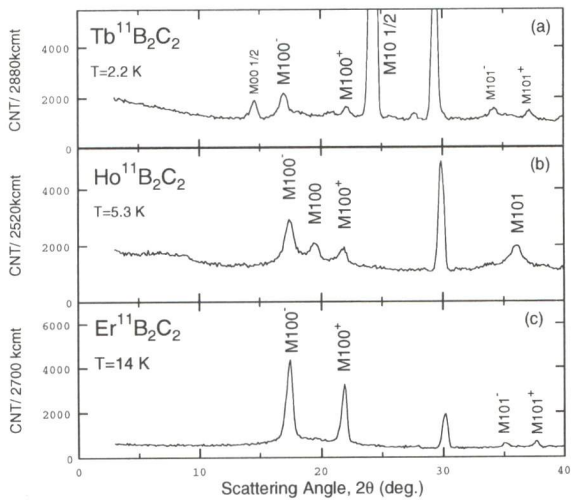


Fig. 2. Powder patterns of $Ho^{11}B_2C_2$ at 5.3 K(a) and $Er^{11}B_2C_2$ at 14.0 K(c) in the incommensurate phases observed on HERMES. The same data of $Tb^{11}B_2C_2$ in Fig. 1(c) is also displayed. Bragg peaks indexed with letter M are magnetic ones.

We would like to thank Mr. K. Nemoto of IMR, Tohoku University for his assistance in the neutron scattering experiments. This work was partially supported by a Grant-in-Aid for Scientific Research(No. 12304017) from the Japan Society for the Promotion of Science.

1) T. Onimaru, H. Onodera, K. Ohoyama, H. Yamauchi and Y. Yamaguchi: J. Phys. Soc. Jpn. **68** (1999) 2287.
2) H. Yamauchi, H. Onodera, K. Ohoyama, T. Onimaru, M. Kosaka, M. Ohashi and Y. Yamaguchi: J. Phys. Soc. Jpn. **68** (1999) 2057.
3) T. Matsumura, S. Nakamura, T. Goto, H. Amitsuka, K. Matsuhira, T. Sakakibara and T. Suzuki: J. Phys. Soc. Jpn. **67** (1998) 612.
4) J.M. Effantin, J. Rossat-Mignot, P. Burlet, H. Bartholin, S. Kunii and T. Kasuya: J. Magn. Magn. Mater **47&48** (1985) 145.
5) Y. Tanaka, T. Inami, T. Nakamura, H. Yamauchi, H. Onodera, K. Ohoyama, Y. Yamaguchi: J. Phys.: Condens. Matter **11** (1999) L505.
6) K. Hirota, T. Matsumura, H. Nakao, Y. Wakabayashi, Y. Murakami and Y. Endoh: Phys. Rev. Lett. **84** (2000) 2706.
7) H. Onodera, H. Yamauchi and Y. Yamaguchi: J. Phys. Soc. Jpn. **68** (1999) 2526.
8) K. Ohoyama, H. Yamauchi, A. Tobo, H. Onodera, H. Kadowaki and Y. Yamaguchi: J. Phys. Soc. Jpn. **69** (2000) 3401.
9) K. Ohoyama T. Onimaru, H. Onodera, H. Yamauchi and Y. Yamaguchi: J. Phys. Soc. Jpn. **69** (2000) 2623.
10) K. Ohoyama, T. Kanouchi, K. Nemoto, M. Ohashi, T. Kajitani and Y. Yamaguchi: Jpn. J. Appl. Phys. **37** (1998) 3319.
11) H. Onodera, K. Kaneko, T. Onimaru, K. Ohoyama, Y. Yamaguchi, H. Kobayashi, Y. Nemoto and T. Goto: submitted to J. Magn. Magn. Mater.
12) A. Tobo, H. Yamauchi, H. Onodera, K. Ohoyama and Y. Yamaguchi: submitted to J. Phys. Soc. Jpn. Suppl.
13) K. Kaneko, K. Ohoyama, A. Tobo, H, Yamauchi, H. Onodera and Y. Yamaguchi: submitted to J. Phys. Soc. Jpn. Suppl.
14) unpublished.